Dyes and Pigments 195 (2021) 109745

Contents lists available at ScienceDirect

Dyes and Pigments

journal homepage: www.elsevier.com/locate/dyepig

Unexpected effect of iodine atoms in heptamethine cyanine dyes on the photodynamic eradication of Gram-positive and Gram-negative pathogens

Olga Semenova [a,b], Dmytro Kobzev [a,b], Fares Yazbak [c], Faina Nakonechny [c], Olga Kolosova [b], Anatoliy Tatarets [b], Gary Gellerman [a], Leonid Patsenker [a,*]

[a] Department of Chemical Sciences, Ariel University, Ariel, Israel
[b] SSI "Institute for Single Crystals" of the National Academy of Sciences of Ukraine, Kharkiv, Ukraine
[c] Department of Chemical Engineering, Ariel University, Ariel, Israel

ARTICLE INFO

Keywords:
Iodinated cyanines
Photosensitizers
Antimicrobial photodynamic therapy
Aggregation

ABSTRACT

The introduction of heavy atoms such as iodine into organic dye molecules is known to improve the efficacy of photodynamic therapy (PDT) in general and antimicrobial photodynamic therapy (APDT) in particular. Such a phenomenon is attributed to the increasing probability of spin–orbit coupling resulting in the elevated rates of reactive species generation. In this work, we synthesize a series of novel, near-IR, iodinated heptamethine cyanine dyes containing carboxylic function and report on the unexpected effect of the increasing number of iodine atoms (up to six) on the photodynamic eradication of Gram-positive (*Staphylococcus aureus*) and Gram-negative (*Escherichia coli* and *Pseudomonas aeruginosa*) microbial pathogens. The efficacy of *S. aureus* photoeradication by non-charged, zwitterionic cyanines increases with increasing the number of iodine atoms up to two, remains almost unchanged for the two-, three- and four-iodinated dyes, and reduces in the case of the hexaiodinated cyanine. However, the mono-iodinated dye exhibits the most pronounced phototoxic effect to *E. coli* and *P. aeruginosa*. An additional positive charge provided by a triethylammonium group decreases photokilling of *S. aureus* but improves inactivation of *E. coli* and *P. aeruginosa*.

1. Introduction

Organic photosensitizing dyes are used in photodynamic antimicrobial therapy (APDT) [1], also called photodynamic antimicrobial chemotherapy (PACT) [2], for killing pathogenic bacteria [3], as well as in photodynamic therapy (PDT) of cancer [4,5] and for eradication of viruses [6] and fungi [7]. The clinically approved photosensitizers are in general porphyrins, which absorb light in the short wavelength range and to a lesser extent in the red and near-IR spectrum region [8,9]. Among the most potent non-porphyrin based photosensitizers are phthalocyanines [10–12] and cyanines [13,14]. One example of cyanine based photosensitizers is indocyanine green (**ICG**) approved by the U.S. Food and Drug Administration (FDA) and European Medicines Agency for photodynamic treatment of several kinds of cancer [15,16].

Due to the high extinction coefficients (up to 250,000 $M^{-1}cm^{-1}$) within the optical therapeutic window, the long-wavelength absorbing and emitting cyanine dyes, in particular heptamethine cyanines are considered promising tools for bioimaging, photodynamic therapy, and theranostic applications [17]. The chemical structures of cyanines can be relatively easy modified to adjust their absorption and emission maxima, solubility, hydrophobic-hydrophilic properties, and to introduce reactive groups facilitating further linkage to biomolecules and target specific carriers [18]. Some cyanines were reported to exhibit a pronounced phototoxicity [19]. In recent years, there has been growing interest, therefore, to cyanine dyes as potential photosensitizers [20].

The introduction of heavy atoms such as iodine into the organic dye molecules is known to improve efficacy of PDT [21,22] and APDT [23–25], which is attributed to the increasing probability of spin-orbit coupling and triplet state population resulting in the elevated rates of reactive species generation [26,27]. This effect has recently been noted for cyanine dyes [28,29] among others [30].

Here, we synthesize a series of novel iodinated heptamethine cyanine dyes containing carboxylic groups (Fig. 1) that can be further utilized for binding to target-specific carriers. These dyes are investigated for photodynamic eradication of representative Gram-positive (*Staphylococcus aureus*) and Gram-negative (*Escherichia coli* and *Pseudomonas*

* Corresponding author. Department of Chemical Sciences, Ariel University, Ariel, 40700, Israel.
E-mail addresses: olga.semenova@isc.kh.ua (O. Semenova), kobzev@isc.kh.ua (D. Kobzev), faresy@ariel.ac.il (F. Yazbak), fainan@ariel.ac.il (F. Nakonechny), kolosova@isc.kh.ua (O. Kolosova), tatarets@isc.kh.ua (A. Tatarets), garyg@ariel.ac.il (G. Gellerman), leonidpa@ariel.ac.il (L. Patsenker).

https://doi.org/10.1016/j.dyepig.2021.109745
Received 8 July 2021; Received in revised form 21 August 2021; Accepted 22 August 2021
Available online 26 August 2021

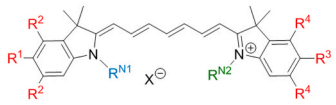

Dye	R^{N1}	R^{N2}	X	R^1	R^2	R^3	R^4
Cy7	Me	$(CH_2)_5COO^-$	–	H	H	H	H
1ICy7	Me	$(CH_2)_5COO^-$	–	I	H	H	H
2ICy7	Me	$(CH_2)_5COO^-$	–	I	H	I	H
2ICy7+	$(CH_2)_3NEt_3^+$	$(CH_2)_5COO^-$	CF_3COO^-	I	H	I	H
3ICy7	Me	$(CH_2)_5COO^-$	–	I	I	H	H
4ICy7	Me	$(CH_2)_5COO^-$	–	I	I	I	H
6ICy7	Me	$(CH_2)_5COO^-$	–	I	I	I	I

Fig. 1. Heptamethine cyanine dyes synthesized and investigated in this work.

aeruginosa) pathogens in comparison with the non-iodinated analog, **Cy7**.

2. Experimental

2.1. General

All chemicals were supplied by Alfa Aesar Israel and Sigma-Aldrich. Solvents were purchased from Bio-Lab Israel and used as is. Chemical reactions were monitored by TLC (Silica gel 60 F-254, Merck) and LC/MS.

LC/MS analysis was performed using an Agilent Technologies 1260 Infinity (LC) 6120 quadrupole (MS), column Agilent Zorbax SB-C18, 1.8 mm, 2.1 × 50 mm, column temperature 50 °C, eluent water-acetonitrile (ACN) + 0.1% formic acid.

HRMS was performed in ESI positive mode by using an Agilent 6550 iFunnel Q-TOF LC/MS instrument.

^{1}H NMR and ^{13}C NMR spectra were recorded on a Bruker Avance III HD (^{1}H 400 MHz and ^{13}C 100 MHz) spectrometer and a BBO probe equipped with a Z gradient coil. ^{1}H NMR spectra of quaternized indolenines **1a-1d** and **3a-3c** (all of them were recently reported) were measured in DMSO-d_6 at 300K. ^{1}H NMR and ^{13}C NMR spectra of heptamethine cyanine dyes **Cy7, 1ICy7–6ICy7** were measured in a $CDCl_3$ (80%) – CD_3OD (20%) mixture at 275K.

2.2. Synthesis

1,2,3,3-Tetramethyl-3*H*-indol-1-ium iodide (1a), 5-iodo-1,2,3,3-tetramethyl-3*H*-indol-1-ium iodide (1b) and **4,5,6-triiodo-1,2,3,3-tetramethyl-3*H*-indol-1-ium iodide (1c) were synthesized by the reported procedures [9,10] .**

1,2,3,3-Tetramethyl-3*H*-indol-1-ium iodide (1a): Yield: 74%. ^{1}H NMR (400 MHz, DMSO-d_6, ppm): δ 7.91 (d, J = 5.2 Hz, 1H), 7.83 (d, J = 5.4 Hz, 1H), 7.62 (t, J = 3.6 Hz, 2H), 3.98 (s, 3H), 2.77 (s, 3H), 1.53 (s, 6H). MS m/z (ESI$^+$) $C_{12}H_{16}IN$ calculated $[M\text{-}I^-]^+$ 174.13, found m/z 174.10.

5-Iodo-1,2,3,3-tetramethyl-3*H*-indol-1-ium iodide (1b): Yield: 73%. ^{1}H NMR (400 MHz, DMSO-d_6, ppm): δ 8.27 (s, 1H), 7.99 (d, J = 8.5 Hz, 1H), 7.71 (d, J = 8.4 Hz, 1H), 3.93 (s, 3H), 2.73 (s, 3H), 1.51 (s, 6H). MS m/z (ESI$^+$) $C_{12}H_{15}I_2N$ calculated $[M\text{-}I^-]^+$ 300.02, found m/z 300.16.

4,5,6-Triiodo-1,2,3,3-tetramethyl-3*H*-indol-1-ium iodide (1c): Yield: 43%. ^{1}H NMR (400 MHz, DMSO-d_6, ppm): δ 8.52 (s, 1H), 3.92 (s, 3H), 2.76 (s, 3H), 1.59 (s, 6H). MS m/z (ESI$^+$) $C_{12}H_{13}I_4N$ calculated $[M\text{-}I^-]^+$ 551.82, found m/z 551.80.

5-Iodo-2,3,3-trimethyl-1-(3-(triethylammonio)propyl)-3*H*-indol-1-ium dibromide (1d): 5-Iodo-2,3,3-trimethyl-3*H*-indole (1.0 g, 3.5 mmol) and 3-bromo-*N*,*N*,*N*-triethylpropan-1-aminium bromide (1.23 g, 3.9 mmol) were stirred in acetonitrile (14 mL) at reflux for 2 days. Reaction mixture was diluted with benzene (50 mL). In 1 h the solvent was decanted and the viscous solid was triturated with diethyl ether, filtered, washed with ether, and dried to yield **1d** (0.6 g, 29%). ^{1}H NMR (400 MHz, DMSO-d_6, ppm): δ 8.33 (s, 1H), 8.04 (d, J = 7.8 Hz, 1H), 7.95 (d, J = 7.6 Hz, 1H), 4.56 (t, J = 7.7 Hz, 2H), 3.25 (m, 8H), 2.91 (s, 3H), 2.18 (m, 2H), 1.56 (s, 6H), 1.18 (t, J = 7.3 Hz, 9H). MS m/z (ESI$^+$) $C_{20}H_{33}Br_2IN_2$ calculated $[M - 2Br]^+$ 428.17, found m/z 428.20.

1-(5-Carboxypentyl)-2,3,3-trimethyl-3*H*-indol-1-ium bromide (3a): 2,3,3-Trimethyl-3*H*-indole (1.0 g, 6.3 mmol) was mixed with 6-bromohexanoic acid (1.84 g, 9.4 mmol) and heated at 120 °C for 15 h in a sealed tube. The reaction mixture was cooled to RT, diluted with benzene (5 mL), the solvent was decanted, and the residue was triturated with benzene (3 × 5 mL), and filtered. The obtained precipitate was washed with acetone (1 mL) and dried to yield **3a** (1.33 g, 60%). ^{1}H NMR (400 MHz, DMSO-d_6, ppm): δ 7.97 (d, J = 5.1 Hz, 1H), 7.84 (d, J = 3.4 Hz, 1H), 7.62 (t, J = 4.1 Hz, 2H), 4.45 (t, J = 7.8 Hz, 2H), 2.84 (s, 3H), 2.23 (t, J = 7.2 Hz, 2H), 1.85 (m, 2H), 1.56 (m, 2H), 1.54 (s, 6H), 1.43 (m, 2H). MS m/z (ESI$^+$) $C_{17}H_{24}BrNO_2$ calculated $[M - Br]^+$ 274.18, found m/z 274.20.

1-(5-Carboxypentyl)-5-iodo-2,3,3-trimethyl-3*H*-indol-1-ium bromide (3b) was obtained by the same procedure as for **3a** starting from 5-iodo-2,3,3-trimethyl-3*H*-indole (1.0 g, 3.5 mmol) and 6-bromohexanoic acid (1.37 g, 7.0 mmol) by heating at 90 °C for 2 days in a sealed tube. Yield: 0.81 g (48%). ^{1}H NMR (400 MHz, DMSO-d_6, ppm): δ 8.31 (s, 1H), 7.99 (d, J = 8.4 Hz, 1H), 7.81 (d, J = 8.5 Hz, 1H), 4.43 (t, J = 7.7 Hz, 2H), 2.82 (s, 3H), 2.20 (t, J = 6.7 Hz, 2H), 1.82 (m, 2H), 1.53 (s, 6H), 1.42 (m, 2H), 1.34 (m, 2H). MS m/z (ESI$^+$) $C_{17}H_{23}BrINO_2$ calculated $[M - Br]^+$ 400.08, found m/z 400.12.

1-(5-Carboxypentyl)-4,5,6-triiodo-2,3,3-trimethyl-3*H*-indol-1-ium bromide (3c) was obtained by the same procedure as for **3a** starting from 4,5,6-triiodo-2,3,3-trimethyl-3*H*-indole (1.0 g, 1.9 mmol) and 6-bromohexanoic acid (0.73 g, 3.7 mmol) by heating at 90 °C for 3 days in a sealed tube. Yield 0.4 g (29%). ^{1}H NMR (400 MHz, DMSO-d_6, ppm): δ 8.60 (s, 1H), 4.41 (t, J = 7.7 Hz, 2H), 2.83 (s, 3H), 2.20 (t, J = 6.7 Hz, 2H), 1.79 (m, 2H), 1.60 (s, 6H), 1.51 (m, 2H), 1.44 (m, 2H). MS m/z (ESI$^+$) $C_{17}H_{21}BrI_3NO_2$ calculated $[M - Br]^+$ 651.87, found m/z 651.90.

2.2.1. General procedure for the synthesis of the dyes Cy7, 1ICy7–6ICy7

A solution of indolenine **1a–1d** (0.25 mmol, 1.1 equiv.) and *N*-[5-(phenylamino)-2,4-pentadienylidene]aniline hydrochloride (0.23 mmol, 1.0 equiv.) in acetic anhydride (2 mL) was heated at 90 °C for 15 min to form the corresponding intermediate product **2a–2d**. Then, the second indolenine **3a–3c** (0.25 mmol, 1.1 equiv.) was added and dissolved in the reaction mixture at 90 °C. The reaction mixture was then cooled to 50 °C, pyridine (1 mL) was added, heated at 90 °C for 5 min, and the obtained dye was precipitated with ether, filtered, and washed with ether. The raw product was column purified on Silica gel 60 using 5–10% methanol–chloroform as eluent.

6-(3,3-Dimethyl-2-(7-(1,3,3-trimethylindolin-2-ylidene)hepta-1,3,5-trien-1-yl)-3*H*-indol-1-ium-1-yl)hexanoate (Cy7). Dye **Cy7** was synthesized from 1,2,3,3-tetramethyl-3*H*-indol-1-ium iodide (**1a**) (75 mg, 0.25 mmol), *N*-[5-(phenylamino)-2,4-pentadienylidene]aniline hydrochloride (64 mg, 0.23 mmol), and 1-(5-carboxypentyl)-2,3,3-trimethyl-3*H*-indol-1-ium bromide (**3a**) (88.5 mg, 0.25 mmol). Yield: 119 mg (52%). ^{1}H NMR (400 MHz, $CDCl_3$–CD_3OD, ppm): δ 7.71 (t, J = 13.1 Hz, 2H), 7.42 (t, J = 12.7 Hz, 1H), 7.40–7.34 (m, 2H), 7.32 (d, J = 7.5 Hz, 2H), 7.18 (t, J = 7.4 Hz, 2H), 7.08 (d, J = 8.4 Hz, 1H), 7.06 (d, J = 8.4 Hz, 1H), 6.47 (t, J = 12.5 Hz, 2H), 6.08 (d, J = 13.4 Hz, 1H), 6.05 (d, J = 13.6 Hz, 1H), 3.92 (t, J = 7.4 Hz, 2H), 3.53 (s, 3H), 2.27 (t, J = 7.2

Hz, 2H), 1.84–1.67 (m, 2H), 1.62 (s, 12H), 1.67–1.53 (m, 2H), 1.50–1.35 (m, 2H). ^{13}C NMR (100 MHz, $CDCl_3$–CD_3OD, ppm): δ 175.63 (COOH), 171.14 (CN Ind), 170.56 (CN Ind) 155.75 (CH), 150.53 (2CH), 141.67 (Ar), 141.00 (Ar), 139.80 (Ar), 139.63 (Ar), 127.84 (2CH Ar), 124.76 (2CH), 124.26 (2CH Ar), 121.36 (CH Ar(, 121.23 (CH Ar), 109.50 (CH Ar), 109.40 (CH Ar), 102.68 (CH), 102.42 (CH), 48.47 (2$\underline{C}(CH_3)_2$), 43.09 (CH_2), 32.98 (CH_2), 30.23 (CH_3), 26.83 (4CH_3), 26.19 (CH_2), 25.45 (CH_2), 23.58 (CH_2). HRMS *m/z* (ESI^+) $C_{34}H_{40}N_2O_2$ calculated $[M+H]^+$ 509.3090 (509.3163), found *m/z*: 509.3168.

6-(2-(7-(5-iodo-1,3,3-trimethylindolin-2-ylidene)hepta-1,3,5-trien-1-yl)-3,3-dimethyl-3*H*-indol-1-ium-1-yl)hexanoate (1ICy7). Dye **1ICy7** was synthesized from 5-iodo-1,2,3,3-tetramethyl-3*H*-indol-1-ium iodide (**1b**) (106.75 mg, 0.25 mmol), *N*-[5-(phenylamino)-2,4-pentadienylidene]aniline hydrochloride (64 mg, 0.23 mmol), and 1-(5-carboxypentyl)-2,3,3-trimethyl-3*H*-indol-1-ium bromide (**3a**) (88.5 mg, 0.25 mmol). Yield: 74 mg (45%). ^{1}H NMR (400 MHz, $CDCl_3$–CD_3OD, ppm): δ 7.76 (t, J = 13.1 Hz, 1H), 7.61 (t, J = 13.1 Hz, 1H), 7.59 (d, J = 8.5 Hz, 1H), 7.54 (s, 1H), 7.40 (t, J = 12.7 Hz, 1H), 7.37 (t, J = 7.9 Hz, 1H), 7.36 (d, J = 7.8 Hz, 1H), 7.25 (t, J = 7.4 Hz, 1H), 7.15 (d, J = 7.9 Hz, 1H), 6.77 (d, J = 8.4 Hz, 1H), 6.53 (t, J = 13.3 Hz, 1H), 6.44 (t, J = 13.3 Hz, 1H), 6.20 (d, J = 13.5 Hz, 1H), 5.92 (d, J = 13.3 Hz, 1H), 3.99 (t, J = 7.4 Hz, 2H), 3.42 (s, 3H), 2.24 (t, J = 7.2 Hz, 2H), 1.77 (m, 2H), 1.64 (m, 2H), 1.63 (s, 6H), 1.58 (s, 6H), 1.44 (m, 2H). ^{13}C NMR (100 MHz, $CDCl_3$–CD_3OD, ppm): δ 176.41 (COOH), 172.48 (CN Ind), 168.14 (CN Ind), 155.64 (CH), 152.05 (2CH), 148.66 (CH), 141.83 (Ar), 141.46 (Ar), 140.63 (Ar), 140.16 (Ar), 136.45 (CH Ar), 130.15 (CH Ar), 128.06 (CH Ar), 125.46 (CH Ar), 125.20 (CH), 122.42 (CH Ar), 110.53 (CH Ar), 110.27 (CH Ar), 104.14 (CH), 101.49 (CH), 86.19 (CI Ar), 48.73 ($\underline{C}(CH_3)_2$), 47.05 ($\underline{C}(CH_3)_2$), 43.54 (CH_2), 33.74 (CH_2), 29.95 (CH_3), 26.86 (2CH_3), 26.67 (2CH_3), 26.35 (CH_2), 25.42 (CH_2), 23.80 (CH_2). HRMS *m/z* (ESI^+) $C_{34}H_{39}IN_2O_2$ calculated $[M+H]^+$ 635.2056 (635.2129), found *m/z*: 635.2134.

6-(5-Iodo-2-(7-(5-iodo-1,3,3-trimethylindolin-2-ylidene)hepta-1,3,5-trien-1-yl)-3,3-dimethyl-3*H*-indol-1-ium-1-yl)hexanoate (2ICy7). Dye **2ICy7** was synthesized from 5-iodo-1,2,3,3-tetramethyl-3*H*-indol-1-ium iodide (**1b**) (106.5 mg, 0.25 mmol), *N*-[5-(phenylamino)-2,4-pentadienylidene]aniline hydrochloride (64 mg, 0.23 mmol), and 1-(5-carboxypentyl)-5-iodo-2,3,3-trimethyl-3*H*-indol-1-ium bromide (**3b**) (120 mg, 0.25 mmol). Yield: 65 mg (38%). ^{1}H NMR (400 MHz, $CDCl_3$–CD_3OD, ppm): δ 7.71 (t, J = 13.0 Hz, 2H), 7.63 (d, J = 8.3 Hz, 2H), 7.60 (s, 2H), 7.45 (t, J = 12.7 Hz, 1H), 6.87 (d, J = 8.2 Hz, 1H), 6.85 (d, J = 8.1 Hz, 1H), 6.51 (t, J = 12.1 Hz, 2H), 6.08 (d, J = 12.7 Hz, 1H), 6.06 (d, J = 13.5 Hz, 1H), 3.90 (t, J = 7.2 Hz, 2H), 3.49 (s, 3H), 2.23 (t, J = 7.2 Hz, 2H), 1.72 (m, 2H), 1.64 (m, 2H), 1.60 (s, 12H), 1.42 (m, 2H). ^{13}C NMR (100 MHz, $CDCl_3$–CD_3OD, ppm): δ 176.74 (COOH), 170.26 (CN Ind), 169.74 (CN Ind), 156.26 (CH), 150.81 (CH), 150.69 (CH), 142.00 (Ar), 141.75 (Ar), 141.53 (Ar), 140.86 (Ar), 136.73 (2CH Ar), 130.45 (CH Ar), 130.31 (CH Ar), 125.65 (2CH), 111.38 (CH Ar), 111.25 (CH Ar), 103.08 (CH), 102.86 (CH), 87.63 (CI Ar), 88.52 (CI Ar), 48.2 (2$\underline{C}(CH_3)_2$), 43.18 (CH_2), 33.48 (CH_2), 30.34 (CH_3), 26.78 (4CH_3), 26.12 (CH_2), 25.43 (CH_2), 23.73 (CH_2). HRMS *m/z* (ESI^+) $C_{34}H_{38}I_2N_2O_2$ calculated $[M+H]^+$ 761.1023 (761.1095), found *m/z*: 761.1101.

6-(5-Iodo-2-(7-(5-iodo-3,3-dimethyl-1-(3-(triethylammonio) propyl)indolin-2-ylidene)hepta-1,3,5-trien-1-yl)-3,3-dimethyl-3*H*-indol-1-ium-1-yl)hexanoate trifluoroacetate (2ICy7+). Dye **2ICy7+** was synthesized from 5-iodo-2,3,3-trimethyl-1-(3-(triethylammonio) propyl)-3*H*-indol-1-ium dibromide (**1d**) (147 mg, 0.25 mmol), *N*-[5-(phenylamino)-2,4-pentadienylidene]aniline hydrochloride (65 mg, 0.23 mmol), and 1-(5-carboxypentyl)-5-iodo-2,3,3-trimethyl-3*H*-indol-1-ium bromide (**3b**) (120 mg, 0.25 mmol). The product was purified on a RP18 column (acetonitrile–water + 0.05% TFA). Yield: 34 mg (15%). ^{1}H NMR (400 MHz, $CDCl_3$–CD_3OD, ppm): δ 7.74 (t, J = 13.0 Hz, 1H), 7.70 (d, J = 8.3 Hz, 1H), 7.68 (t, J = 13.0 Hz, 1H), 7.66 (s, 1H), 7.64 (d, J = 8.1 Hz, 1H), 7.59 (s, 1H), 7.40 (t, J = 12.8 Hz, 1H), 7.01 (d, J = 8.3 Hz, 1H), 6.91 (d, J = 8.3 Hz, 1H), 6.60 (t, J = 12.7 Hz, 1H), 6.55 (t, J = 12.8 Hz, 1H), 6.28 (d, J = 13.2 Hz, 1H), 6.15 (d, J = 13.5 Hz, 1H), 4.08 (t, J = 7.0 Hz, 2H), 3.95 (t, J = 6.8 Hz, 2H), 3.43 (t, J = 7.9, 2H), 3.26 (m, 6H) 2.30 (t, J = 7.2 Hz, 2H,), 2.04 (m, 2H), 1.77 (m, 2H), 1.66 (m, 2H), 1.64 (s, 6H), 1.61 (s, 6H), 1.45 (m, 2H), 1.27 (t, J = 7.1 Hz, 9H). HRMS *m/z* (ESI^+) $C_{44}H_{56}F_3I_2N_3O_4$ calculated $[M–CF_3COO]^+$ 888.2451 (888.2445), found *m/z*: 888.2462.

6-(3,3-Dimethyl-2-(7-(4,5,6-triiodo-1,3,3-trimethylindolin-2-ylidene)hepta-1,3,5-trien-1-yl)-3*H*-indol-1-ium-1-yl)hexanoate (3ICy7). Dye **3ICy7** was synthesized from 4,5,6-triiodo-1,2,3,3-tetramethyl-3*H*-indol-1-ium iodide (**1c**) (170 mg, 0.25 mmol), *N*-[5-(phenylamino)-2,4-pentadienylidene]aniline hydrochloride (65 mg, 0.23 mmol), and 1-(5-carboxypentyl)-2,3,3-trimethyl-3*H*-indol-1-ium bromide (**3a**) (88.0 mg, 0.25 mmol). Yield: 75 mg (37%). ^{1}H NMR (400 MHz, $CDCl_3$–CD_3OD, ppm): δ 7.82 (t, J = 12.4 Hz, 1H), 7.54 (t, J = 13.0 Hz, 1H), 7.50 (s, 1H), 7.40 (d, J = 7.7 Hz, 2H), 7.40 (t, J = 12.6 Hz, 1H), 7.31 (t, J = 7.6 Hz, 1H), 7.25 (d, J = 7.8 Hz, 1H), 6.59 (t, J = 12.6 Hz, 1H), 6.43 (t, J = 12.5 Hz, 1H), 6.36 (d, J = 13.5 Hz, 1H), 5.77 (d, J = 13.1 Hz, 1H), 4.07 (t, J = 7.2 Hz, 2H), 3.31 (s, 3H), 2.22 (t, J = 7.2 Hz, 2H), 1.79 (m, 2H), 1.69 (s, 6H), 1.65 (s, 6H), 1.64 (m, 2H), 1.45 (m, 2H). ^{13}C NMR (100 MHz, $CDCl_3$–CD_3OD, ppm): δ 177.20 (COOH), 174.33 (CN Ind), 166.58 (CN Ind), 155.22 (CH), 153.27 (CH), 146.81 (CH), 144.47 (Ar), 141.28 (Ar), 140.59 (Ar), 140.34 (Ar), 128.28 (CH Ar), 126.34 (CH), 126.11 (CH), 125.57 (CH Ar), 121.54 (CH Ar), 118.83 (2CH Ar), 116.77 (CI Ar), 111.04 (2CI Ar), 105.96 (CH), 101.98 (CH), 50.51 ($\underline{C}(CH_3)_2$), 49.30 ($\underline{C}(CH_3)_2$), 44.03 (CH_2), 34.28 (CH_2), 28.73 (CH_3), 26.58 (CH_2), 26.50 (2CH_3), 25.42 (CH_2), 23.98 (CH_2), 23.29 (2CH_3). HRMS *m/z* (ESI^+) $C_{34}H_{37}I_3N_2O_2$ calculated $[M+H]^+$ 886.9989 (887.0062), found *m/z*: 887.0067.

6-(5-Iodo-3,3-dimethyl-2-(7-(4,5,6-triiodo-1,3,3-trimethylindolin-2-ylidene)hepta-1,3,5-trien-1-yl)-3*H*-indol-1-ium-1-yl)hexanoate (4ICy7). Dye **4ICy7** was synthesized from 4,5,6-triiodo-1,2,3,3-tetramethyl-3*H*-indol-1-ium iodide (**1c**) (170 mg, 0.25 mmol), *N*-[5-(phenylamino)-2,4-pentadienylidene]aniline hydrochloride (65 mg, 0.23 mmol), and 1-(5-carboxypentyl)-5-iodo-2,3,3-trimethyl-3*H*-indol-1-ium bromide (**3b**) (120 mg, 0.25 mmol). Yield: 116 mg (50%). ^{1}H NMR (400 MHz, $CDCl_3$–CD_3OD, ppm): δ 7.78 (t, J = 12.8 Hz, 1H), 7.68 (d, J = 8.3 Hz, 1H), 7.66 (s, 1H), 7.63 (t, J = 13.0 Hz, 1H), 7.57 (s, 1H), 7.43 (t, J = 12.7 Hz, 1H), 6.96 (d, J = 8.4 Hz, 1H), 6.58 (t, J = 12.6 Hz, 1H), 6.48 (t, J = 12.6 Hz, 1H), 5.23 (d, J = 13.4 Hz, 1H), 5.88 (d, J = 13.3 Hz, 1H), 3.98 (t, J = 7.8 Hz, 2H), 3.37 (s, 3H), 2.24 (t, J = 7.2 Hz, 2H), 1.74 (m, 2H), 1.70 (s, 6H), 1.62 (s, 6H), 1.52 (m, 2H), 1.42 (m, 2H). ^{13}C NMR (100 MHz, $CDCl_3$–CD_3OD, ppm): δ 177.01 (COOH), 172.11 (CN Ind), 168.49 (CN Ind), 156.17 (CH), 152.62 (CH), 148.84 (CH), 144.13 (Ar), 142.34 (Ar), 141.45 (Ar), 140.42 (Ar), 137.03 (CH Ar), 130.63 (CH Ar), 126.44 (2CH), 119.32 (CH Ar), 118.06 (CI Ar), 112.19 (CH Ar), 105.56 (CI Ar), 104.78 (CH), 102.10 (CI Ar), 101.18 (CH), 89.21 (CI Ar), 50.99 ($\underline{C}(CH_3)_2$), 48.72 ($\underline{C}(CH_3)_2$), 43.70 (CH_2), 33.48 (CH_2), 28.42 (CH_3), 26.60 (2CH_3), 26.38 (CH_2), 25.32 (CH_2), 23.66 (CH_2), 23.16 (2CH_3). HRMS *m/z* (ESI^+) $C_{34}H_{36}I_4N_2O_2$ calculated $[M+H]^+$ 1012.8956 (1012.9028), found *m/z*: 1012.9034.

6-(4,5,6-Triiodo-3,3-dimethyl-2-(7-(4,5,6-triiodo-1,3,3-trimethylindolin-2-ylidene)hepta-1,3,5-trien-1-yl)-3*H*-indol-1-ium-1-yl) hexanoate (6ICy7). Dye **6ICy7** was synthesized from 4,5,6-triiodo-1,2,3,3-tetramethyl-3*H*-indol-1-ium iodide (**1c**) (170 mg, 0.25 mmol), *N*-[5-(phenylamino)-2,4-pentadienylidene]aniline hydrochloride (65 mg, 0.23 mmol), and 1-(5-carboxypentyl)-4,5,6-triiodo-2,3,3-trimethyl-3*H*-indol-1-ium bromide (**3c**) (183 mg, 0.25 mmol). Yield: 78 mg (27%). ^{1}H NMR (400 MHz, $CDCl_3$–CD_3OD, ppm): δ 7.73 (t, J = 13.0 Hz, 2H), 7.65 (s, 1H), 7.62 (s, 1H), 7.45 (t, J = 12.6 Hz, 1H), 6.57 (m, 2H), 6.06 (d, J = 13.5 Hz, 2H), 3.86 (t, J = 7.6 Hz, 2H), 3.47 (s, 3H), 2.26 (t, J = 7.1 Hz, 2H), 1.72 (s, 12H), 1.68 (m, 2H), 1.63 (m, 2H), 1.42 (m, 2H). ^{13}C NMR (100 MHz, $CDCl_3$–CD_3OD, ppm): 177.05 (COOH), 170.80 (2CN Ind), 156.82 (CH), 151.90 (CH), 151.50 (CH), 143.68 (Ar), 142.93 (Ar), 141.94 (Ar), 141.70 (Ar), 120.03 (2CH), 119.95 (2CH Ar), 119.54 (2CI Ar), 105.95 (CI Ar), 105.75 (CI Ar), 102.86 (2CI Ar), 102.45 (CH), 102.22 (CH), 51.72 ($\underline{C}(CH_3)_2$), 51.57 ($\underline{C}(CH_3)_2$), 43.08 (CH_2), 33.57 (CH_2), 28.72 (CH_3), 25.81 (CH_2), 25.22 (CH_2), 23.68 (CH_2), 23.01

($4CH_3$). HRMS *m/z* (ESI^+) $C_{34}H_{34}I_6N_2O_2$ calculated $[M+H]^+$ 1264.6888 (1264.6961), found *m/z*: 1264.6967.

2.3. Absorption and fluorescence measurements

The absorption spectra were recorded on a Jasco V-730 UV–Vis spectrophotometer and the fluorescence spectra were taken on an Edinburgh FS5 spectrofluorometer. The absorption and fluorescence spectra were measured at 25 °C in standard 1-cm quartz cells at ~1 μM dye concentrations in DMSO and 0.9% aqueous saline. The excitation wavelength (λ*) was 680 nm.

To determine the absolute fluorescence quantum yields (F_F), the integrated relative intensities of the dyes were measured *vs.* the commercially available disulfonated **Cy7** (**Zy7**, SETA BioMedicals, https://www.setabiomedicals.com) in phosphate buffer pH 7.4 as the reference (F_F = 13%) [8]; and the quantum yields were calculated according to Equation (1) [31].

$$\Phi_F = \Phi_{FRef} \times (F / F_{Ref}) \times (A_{Ref} / A) \times (n_{D(media)}{}^2 / n_{D(Ref)}{}^2), \quad (1)$$

where Φ_{FRef} is the quantum yield of the reference, F_{Ref} and F are the areas (integral intensities) of the emission spectra ($F = \int I(\lambda)d\lambda$) of the reference dye and the dye under examination, A_{Ref} and A, are the absorbances at the excitation wavelength of the reference dye and the dye under examination, and $n_{D(Ref)}$ and $n_{D(media)}$ are the refractive indices of the solvents used for the reference dye and the dye under examination.

The quantum yield for each dye was independently measured three times and the average value was taken.

2.4. Quantum yield of singlet oxygen formation

The quantum yields of the singlet oxygen formation were measured according to the known procedure [32]. A solution of 1,3-diphenylisobenzofuran (**DPBF**, $c \sim 1.4 \times 10^{-5}$ M) and a dye under investigation ($c \sim 5–7 \times 10^{-6}$ M) in methanol was prepared. The obtained solution (3.0 mL) was light irradiated by a 747 nm 1 W LED in a standard 1 cm quartz cell with stirring (LED was located in 1 mm distance from the cell wall) and the absorption spectra were recorded over time. The total irradiation time was in the range of 20–120 min. During this time the absorbance of DPBF reduced to about 10% of its initial value. The corresponding plot representing the absorbance of DPBF at 411 nm *versus* time was drawn and fitted by first-order exponential decay function. Then, the singlet oxygen formation quantum yield Φ_Δ was calculated relative to 1,1′,3,3,3′,3′-hexamethylindotricarbocyanine iodide (**HITC**) (Φ_Δ = 0.0089 [32]) according to Equation (2).

$$\Phi_\Delta = \Phi_{\Delta Ref} \times (k / k_{Ref}) \times (A_{Ref} / A), \quad (2)$$

where $\Phi_{\Delta Ref}$ is the quantum yield of the singlet oxygen formation for the reference dye (**HITC**), k_{Ref} and k are the rates of **DPBF** degradation obtained from the corresponding fitting curves of the reference dye and the dye under examination, and A_{Ref} and A are the absorbances at the excitation wavelength (747 nm) of the reference dye and the dye under examination. Each experiment was carried out in triplicate and the average Φ_Δ was taken. The reproducibility in the determination of Φ_Δ was no worse that 5%.

2.5. Antimicrobial studies

Cultures of *S. aureus* (ATCC 25923), *E. coli* (ATCC 25922) and *P. aeruginosa* (ATCC 25668) were grown on Brain Heart agar plates (BHA, Acumedia, Lansing, MI, USA) for 24 h, transferred into Brain Heart broth (BH, Acumedia, Lansing, MI, USA), grown at 37 ± 1 °C with shaking at 170 rpm until reaching the absorbance A = 0.10 ± 0.02 at 660 nm, which corresponded to a final concentration of 10^8 cells/mL, and diluted with commercially available sterile 0.9% saline solution to the final concentration of 10^3–10^4 cells/mL.

All preparatory operations with photosensitizers were carried out in the dark to avoid their activation and photobleaching. The stock solutions of the dyes in DMSO (3–8 mM, spectrophotometrical control by known dilutions) were prepared and the desirable final concentrations were prepared in up to three dilutions. Then, each dye solution in DMSO (7 μL) was added to bacterial suspensions (1 mL) in 0.9% saline (Falcon® 24-well polystyrene clear flat bottom plate was used). Thus, the amount of DMSO added to the bacterial suspensions was always 0.7% (7% was used in several experiments, as noted below). The bacterial suspensions were then incubated in the dark at RT for 30 min and then exposed to light with shaking (or kept in the dark for the control) for certain periods of time according to the experimental conditions. The light exposure was carried out by a 730-nm, 30 W LED equipped with a 60° lens from the distance of 8 cm (light power density 56 mW/cm^2).

After the light exposure, aliquots of each sample (100 μL) were spread over BHA plates with a Drigalsky spreader, incubated at 37 °C for 24 h, and the colony forming units (CFU) were counted using a colony counter Scan 500 (Interscience, Saint-Nom-la-Bretèche, France).

To verify the dark toxicity of the dyes, the same experiments were carried out in parallel without light exposure. As the control we utilized the samples of bacteria without dye: (i) in the dark and without DMSO, (ii) in the dark in the presence of DMSO, (iii) exposed to light without DMSO, and (iv) exposed to light in the presence of DMSO.

All the experiments with bacteria were carried out in triplicate 4–5 times in different days and the average values were taken.

3. Results and discussion

3.1. Overview of the dye structures

We synthesized a series of indolenine based heptamethine cyanine dyes of asymmetric structure containing no iodine (**Cy7**) as well as one (**1ICy7**), two (**2ICy7**), three (**3ICy7**), four (**4ICy7**) and six (**6ICy7**) iodine atoms. These dyes possess a carboxypentyl group attached to the nitrogen of one indolenine moiety and methyl group at the second indolenine nitrogen. When the carboxylic group is deprotonated, these dyes exist in zwitterionic form. Furthermore, one of the dyes (**2ICy7**+) bears an additional positive charge provided by the quaternized propyl triethylaminium group substituting N-methyl.

3.2. Synthesis

All the dyes were synthesized by the same approach consisted in a one-pot sequential reaction of *N*-[5-(phenylamino)-2,4-pentadienylidene]aniline hydrochloride with the first and then the second quaternized indolenine (Scheme 1). In the first step, the starting aniline was condensed in acetic anhydride with the first indolenine molecule **1a–1d** to form a corresponding *N*-phenylacetamide derivative **2a–2d**, which was further reacted with the second molecule, *N*-carboxypentyl indolenine **3a–3c** in the presence of pyridine to give the dyes **Cy7**, **1ICy7–6ICy7**, and **2ICy7**+, respectively, in moderate yields (15–52%).

3.3. Spectral properties and quantum yields of singlet oxygen formation

The absorption and emission spectra and the extinction coefficients (ε) of the obtained heptamethine cyanines were measured at the dye concentration $c_{Dye} \sim 1$ μM in DMSO and aqueous saline (Figs. S1 and S2) and the corresponding characteristics are given in Table 1. These dyes absorb in the near-IR, biologically transparent spectral region with the high extinction coefficients ($\varepsilon \sim$ 144,000–176,000 $M^{-1}cm^{-1}$), which is beneficial for applications in the body. The difference in the extinction coefficients between the dyes does not exceed ~20%. There is a tendency that the iodination of the parent dye **Cy7** results in a moderate red-shift in the absorption (up to 18 nm for hexa-iodinated **6ICy7** in DMSO) and a slight increase in the extinction coefficients.

The fluorescence quantum yield (Φ_F) of the dyes measured in DMSO

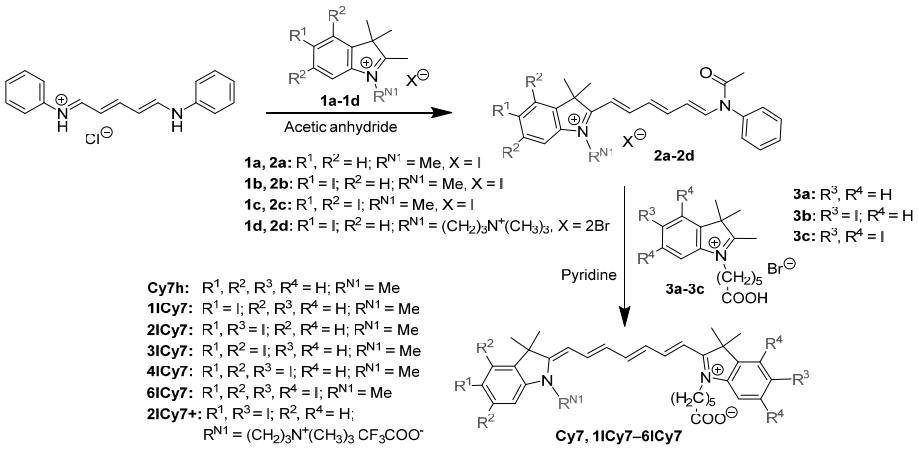

Scheme 1. Synthesis of heptamethine cyanine dyes.

Table 1
Spectral characteristics of cyanine dyes measured at c_{Dye} ~1 μM.

Dye	Structure	DMSO				0.7% DMSO in saline			MeOH
		λ_{max}Ab, nm	ε, $M^{-1}cm^{-1}$	λ_{max}Fl, nm	Φ_F, %	λ_{max}Ab,nm	λ_{max}Fl, nm	Φ_F, %	Φ_Δ, %
Cy7	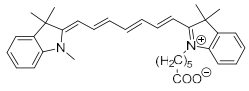	753	143,300	786	55	739	768	13	1.1
1ICy7	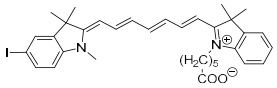	759	168,000	792	53	746	776	12	1.9
2ICy7	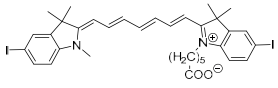	766	173,000	801	55	754	783	4	2.3
2ICy7+	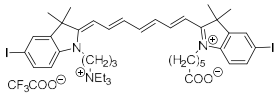	766	176,000	801	48	752	785	10	2.3
3ICy7	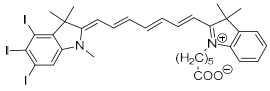	760	148,000	794	49	677[a], 744	774	0.8	2.4
4ICy7	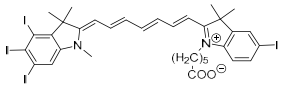	768	144,000	803	48	688[a]	779	0.1	3.7
6ICy7	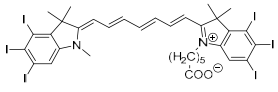	771	166,000	804	52	718[a], 777[a]	779	0.02	7.8

[a] Aggregation band.

(~48–55%) is substantially reduced in aqueous saline (0.02–13%), which can be attributed to the dye aggregation [33–35]. The aggregation bands are well recognized in the absorption spectra (Fig. S2). In the saline solutions, a drastic (~650-fold) decrease of the quantum yield with increasing the number of iodine atoms is observed. In general, such an effect is known to be connected with the increasing probability of

spin–orbit coupling caused by heavy atoms, which results in the growing population of the triplet state and the fluorescence quenching. However, for the investigated cyanine dyes, the decrease of the quantum yield is observed only in the aqueous solutions but not in DMSO. That is, the decrease is associated with the dye aggregation rather than with the heavy atom effect.

All the dyes except **2ICy7+** contain a delocalized positive charge and a localized negative charge on the deprotonated carboxylic group. Therefore, due to the slightly polar structure, these dyes are only a little soluble in saline. The introduction of iodine atoms in the organic compounds is known to reduce their solubility in aqueous media. Thus, the solubility of dimethylaniline in water at 25 °C is 1 g/L [36] while for 4-iodo-dimethylaniline it is 34.64 mg/L [37]. The solubility of benzoic acid in water is 3.44 g/L [38] while for 4-iodobenzoic acid it is 0.04 g/L [39] and only 0.036×10^{-3} g/L for 2,3,5-triiodobenzoic acid [40]. Hereby, the solubility of the investigated dyes decreases with the increasing the number of iodine atoms and the aggregation accordingly increases (Figs. S2 and a). At the same time, due to the presence of an additional positive charge, dye **2ICy7+** is less aggregative compared to **2ICy7** containing the same number of iodines.

The quantum yields of the singlet oxygen formation (Φ_Δ) was measured in methanol solutions by the decrease of the **DPBF** dye, as described in [32], under the light exposure (747 nm 1 W LED). As anticipated, the Φ_Δ were found to increase with increasing the number of iodine atoms (Table 1). Dyes **2ICy7** and **2ICy7+** both containing two iodines exhibited about the same Φ_Δ. In the dark, no pronounced generation of singlet oxygen was detected: the decrease in the **DPBF** absorbance did not exceed 2% during 15 h. According to the absorption spectra (Fig. S3), almost no aggregation was noted in methanol at the investigated dye concentrations ($c \sim 5–7 \times 10^{-6}$ M).

3.4. Toxicity and phototoxicity of the dyes

All experiments with bacteria were carried out in aqueous saline solution. Commercial 0.9% saline solution, used in this work, is known to be acidic (pH ~ 5.5), which is mostly due to the presence of CO_2 [41]. On the other side, the carboxypentyl group existing in all the investigated dye molecules is more acidic (e.g. the pK_a for pentanoic and hexanoic acids are 4.84 [42] and 4.88 [43], respectively). It means that the carboxylic group is basically deprotonated and the dyes **Cy7**, **1ICy7**, **2ICy7**, **3ICy7**, **4ICy7**, and **6ICy7** exist in saline solution in the non-charged zwitterion form. In contrast, **2ICy7+** has a charge of +1 that is localized on the quaternized triethylammonium group.

To investigate the effect of the dyes on bacteria, stock solutions of the dyes were prepared in DMSO and added to the bacterial suspension in saline in such a way that the concentration of DMSO in the sample was 0.7%. Then the bacterial suspensions were incubated with each dye in the dark for 30 min (pre-irradiation incubation), exposed to light and grown in the dark for 24 h at 37 °C followed by the calculation of the number of bacterial colonies. The dye concentrations and the exposure time were varied for each dye. To verify the dark toxicity of the dyes, the same experiments were carried out in parallel without the light exposure.

As the control, the bacterial suspensions containing no dye were utilized. These controls were kept (i) in the dark without DMSO, (ii) in the dark in the presence of DMSO, (iii) exposed to light without DMSO, and (iv) exposed to light in the presence of DMSO. The amount of DMSO in these control samples was the same as for the dye-stained bacteria. The number of bacterial colonies in each experiment was utilized to calculate the survival percentage as compared to the control. Importantly, no detectable bacteria inhibition was registered for all the above controls (i–iv) and the survival for these samples was taken as 100%.

Then, we found that the investigated dyes have no detectable dark toxicity to Gram-positive (*S. aureus*) and Gram-negative (*E. coli* and *P. aeruginosa*) bacteria at least up to the 1 μM and 50 μM dye concentrations, respectively. The dark toxicities at higher dye concentrations were not studied. In the next step, the experiments were performed with light irradiation at different exposure time using a 730-nm 30 W LED (power density 55 mW/cm^2).

3.4.1. Photodynamic eradication of S. aureus

In our study, the effect on phototoxicity of the three following parameters was investigated: the number of iodine atoms in the dye molecules, the concentration of the dyes, and the light doses. The methodological approach was as follows: The effect of the number of iodine atoms in the dyes was first investigated on Gram-positive bacteria *S. aureus*: (i) at the "medium" (100 J/cm^2) and (ii) "low" (3 J/cm^2) light dose *vs.* the dye concentrations, and (iii) at the constant dye concentrations *vs.* the light dose. The "high" light dose (400 J/cm^2) was not applied in the initial research stage because it caused complete killing of *S. aureus* by all the investigated dyes and, therefore, it was not possible to compare efficacies of these dyes.

Following this approach, the impact of the number of iodine atoms and the dye concentration ($c_{Dye} = 0.01–1$ μM) on the *S. aureus* survival was first investigated at the constant light dose of 100 J/cm^2. The most pronounced and nearly equal phototoxicity was observed for **2ICy7**, **3ICy7** and **4ICy7** that contained 2–4 iodine atoms, while **Cy7**, **1ICy7**, **2ICy7+**, and, surprisingly, **6ICy7** were less effective (Fig. 2). These results allow us to draw several conclusions.

First, the introduction of iodine atoms in the **Cy7** molecule, which is the parent structure for all the iodinated dyes, elevates phototoxicity, which is an anticipated result: one iodine atom in **1ICy7** causes a distinct increase of the phototoxicity but this increase is less pronounced as for the 2–4 iodinated dyes (Fig. 2). Thus, the dyes with 2–4 iodines afford almost total bacteria killing (survival 0–2.1%) at 0.01–1 μM, while **1ICy7** at 0.01 μM is much less phototoxic exhibiting the percentage of survival of 60.8%. Obviously, this result is connected with increasing the number of heavy atoms.

The second conclusion is that increasing the number of iodines from 2 to 4 has almost no effect on the photokilling while the hexa-iodinated dye **6ICy7** surprisingly exhibits a reduced activity (the percentage of survival is 35.6% at 0.01 μM) compared to the 2–4 iodinated dyes (survival 0–2.1%).

Third, the non-delocalized positive charge produced by the triethylammonium group (**2ICy7+** *vs.* **2ICy7**) noticeably decreases the phototoxicity (Fig. 2).

We assume that the above phenomena, i.e. "saturation" and reduction of the bacteria photo-eradication with increasing the number of iodine atoms from 2 to 6, can be attributed to the increasing dye aggregation in aqueous media (Fig. S2) resulting in the decreasing dye uptake (the aggregation reduces both the phototoxicity [17,44] and the above mentioned fluorescence quantum yields [17,18,19]). This conclusion contradicts, however, recently reported findings that iodination of small organic molecules such as 4-amino naphthalimides vice versa causes the increase of the dye uptake by several mammalian cells [45].

To check our assumption that increasing the number of iodine atoms (as well as the positive charge) in the series of the investigated cyanines reduces the dye uptake by *S. aureus* and thus decreases the photokilling effect, we measured the dye uptake and correlated it with the survival percentage. For this purpose, *S. aureus* suspensions in saline (10^3–10^4 cells/mL) were incubated with the dyes (1 μM) for 30 min and the fluorescence intensities of these suspensions were measured. Then, the bacteria were separated from the solvent by centrifugation (10 min, 4,000 rpm), resuspended in saline and the fluorescence intensities were again measured. In these experiments, the effect of light scattering on the relative fluorescence intensities was minimized because the samples contained the same number of cells before and after staining. The dye uptakes quantified as the ratios between the fluorescence intensities for the resuspended bacteria and for the initial suspensions were as follows: **Cy7** (0.85), **1ICy7** (0.28), **2ICy7** (0.98), **2ICy7+** (0.21), **3ICy7** (0.99), **4ICy7** (0.97), and **6ICy7** (0.73). These data indicate that **2ICy7**, **3ICy7**

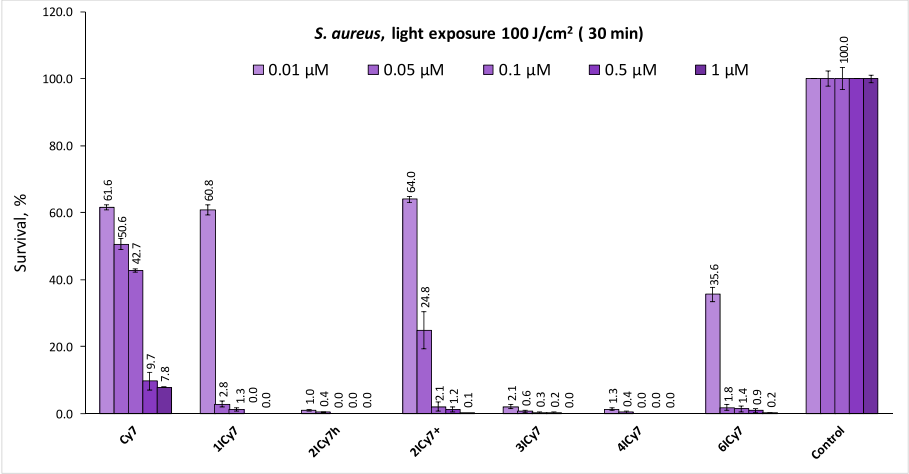

Fig. 2. Survival of *S. aureus* in 0.7% DMSO in saline, when exposed to 100 J/cm^2 light dose (56 mW/cm^2, 30 min) *vs.* the dye concentrations.

and **4ICy7** exhibited the most pronounced uptake while uptake for **6ICy7** and especially for **2ICy7+** was noticeably reduced. The uptake of **Cy7** is lower compared to **2ICy7** but much higher than for **1ICy7**.

The obtained uptake values are in good agreement with the phototoxicities (Fig. 3). Thus, for the iodinated dyes, there is a clear correlation between the uptake and the cell survival ($r = 0.98$). At the same time, the non-iodinated dye **Cy7** exhibits a substantially reduced phototoxicity (elevated survival) compared to the value anticipated from the correlation curve (Fig. 3). More likely, this is due to the fact that the correlation curve takes into account also the contribution of the heavy atom effect.

Furthermore, we studied the effect of the light dose on the dyes' phototoxicity towards *S. aureus* at constant dye concentration of 0.05 μM (Fig. 4). It can be seen that the phototoxicity increases with increasing the light dose from 3 J/cm^2 (1 min) to 400 J/cm^2 (120 min). However, the dyes with two (**2ICy7**) and three (**3ICy7**) iodines almost totally eradicate bacteria even at 3 J/cm^2 and **4ICy7** at 17 J/cm^2. The data presented in Fig. 4 confirm also that the dyes with 2–4 iodines bearing a delocalized positive charge cause the more pronounced bacteria eradication while **1ICy7**, **6ICy7**, **2ICy7+**, and especially **Cy7** are less phototoxic.

It can be seen from Fig. 4 that dyes **2ICy7** and **3ICy7** entirely eradicate *S. aureus* even at a low dye concentration (0.05 μM) and at a very low light dose of 3 J/cm^2. Therefore, we investigated the impact of the dye concentrations on the phototoxicity at this low light dose. Fig. 5 demonstrates that 0.05 μM is, actually, the minimal concentration at which **2ICy7** and **3ICy7** almost completely eradicate *S. aureus* while the dyes with fewer or more iodine atoms are less phototoxic. Thus, the non-charged (zwitterionic) dyes with two and three iodine atoms (**2ICy7** and **3ICy7**) were found to be the most effective against *S. aureus*. They are more effective against this pathogen compared to other dyes at low concentrations and low light doses.

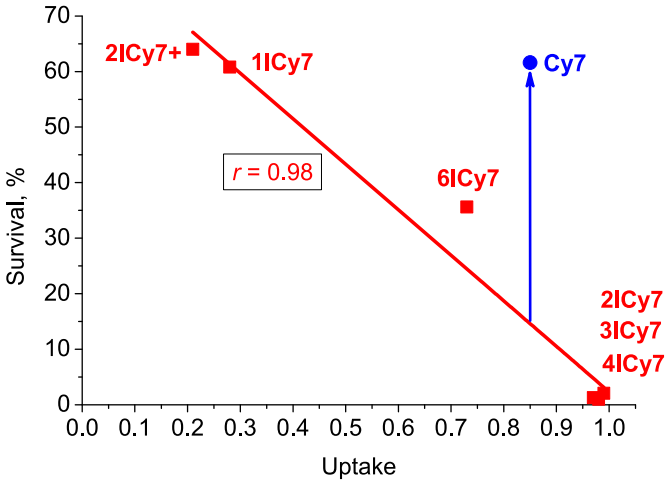

Fig. 3. *S. aureus* survival *vs.* the dye uptake. The uptake was estimated as the ratio between the fluorescence intensities of the stained bacteria after and before washing.

3.4.2. Photodynamic eradication of *E. coli* and *P. aeruginosa*

In the next step, we studied phototoxicity of the dyes towards Gram-negative pathogens *E. coli* and *P. aeruginosa*. The data in Figs. 6–10 show that these bacteria are much more resistant towards photodynamic treatment compared to the Gram-positive *S. aureus*. Thus, all the investigated dyes do not cause a sufficient phototoxic effect to *E. coli* even at 50 μM and light dose of 100 J/cm^2 (Fig. 6). There is a trend, however, that the mono-iodinated **1ICy7** is more active compared to other dyes at 100 J/cm^2 and this tendency is even more pronounced at 200–400 J/cm^2 (Fig. 7). Surprisingly, the dyes containing four and six iodines are less phototoxic than **Cy7**. The increase of the positive charge (**2ICy7+** *vs.* **2ICy7**) has almost no effect on the dye phototoxicity at 100 J/cm^2 (Fig. 6) but noticeably improves the toxic effect at higher light dose of 200–400 J/cm^2 (Fig. 7). Therefore, the mono-iodinated **1ICy7** and positively charged **2ICy7+** are considered more effective against *E. coli* compared to other cyanines.

Similar to *S. aureus*, the decrease in the phototoxicity towards Gram-negative bacteria with increasing the number of iodine atoms between 2 and 6 is supposedly connected with the increasing dye aggregation (Fig. S2) and decreasing dye uptake. The aggregation effect is, however, even more pronounced for Gram-negative bacteria because the dyes are used at much higher concentrations. To diminish the aggregation, we increased the content of DMSO in saline to 10 times, from 0.7% (as in all the above experiments) to 7%. The obtained data in Fig. 8 show that the efficacy of **Cy7**, **1ICy7**, and **2ICy7** to eradicate *E. coli* was noticeably improved. Thus, the survival percentage for these three dyes at 50 μM and 400 J/cm^2 was decreased from 27.6%, 15.4% and 50.0%, respectively, to zero. Nevertheless, the addition of even 7% DMSO to the saline solutions was insufficient to overcome the aggregation and improve the phototoxicity of **3ICy7**, **4ICy7**, and **6ICy7**.

P. aeruginosa was found to be even more resistant towards the investigated dyes than *E. coli* but the same tendency as for *E. coli* was observed: The most phototoxic dyes are mono-iodinated **1ICy7** and positively charged **2ICy7+** (Figs. 9 and 10), which is different from *S. aureus*, where the most phototoxic are the diiodinated (**2ICy7**) and triiodinated (**3ICy7**) cyanines.

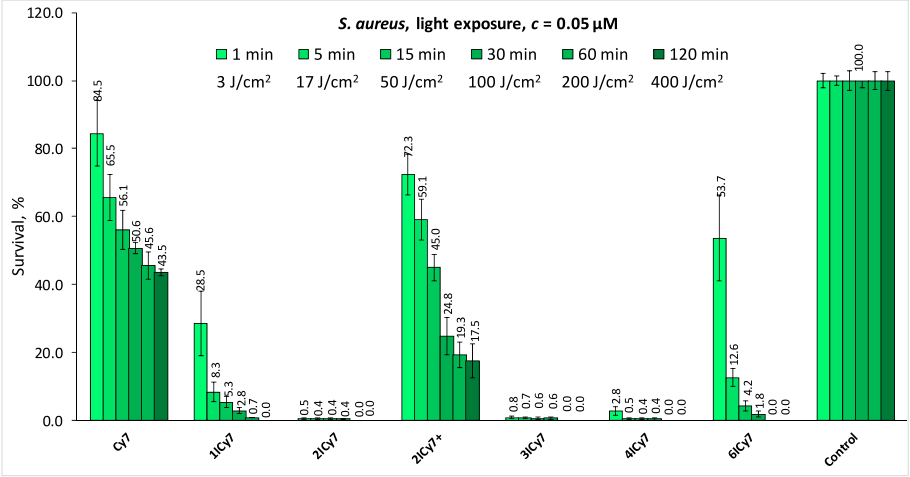

Fig. 4. Survival of *S. aureus* at 0.05 μM dye concentrations in 0.7% DMSO in saline, when exposed to 3 J/cm^2 (1 min), 17 J/cm^2 (5 min), 50 J/cm^2 (15 min), 100 J/cm^2 (30 min), 200 J/cm^2 (60 min), and 400 J/cm^2 (120 min) light doses.

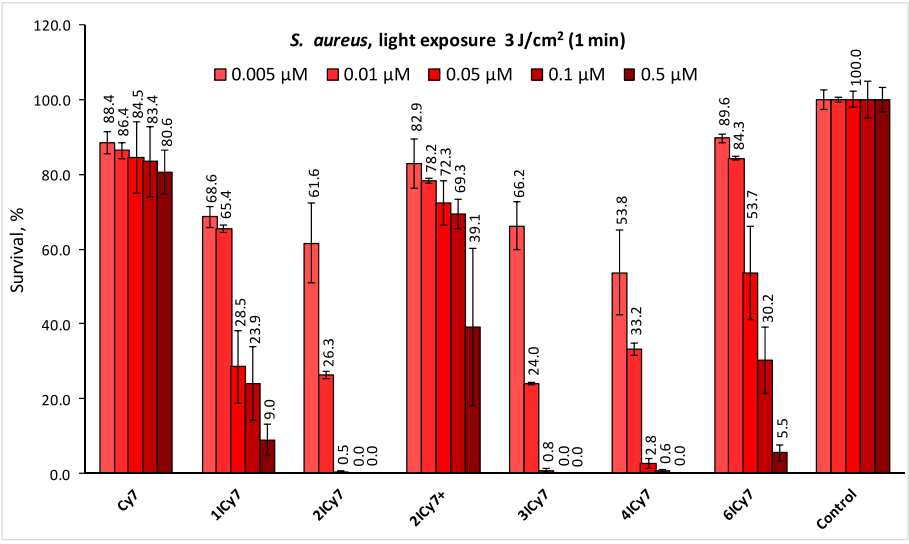

Fig. 5. Survival of *S. aureus* in 0.7% DMSO in saline, when exposed to 3 J/cm^2 light dose (56 mW/cm^2, 1 min) *vs.* the dye concentrations.

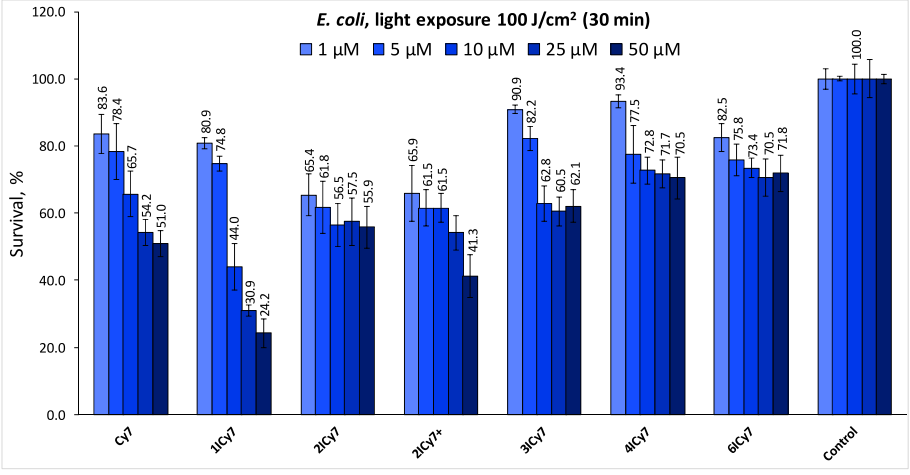

Fig. 6. Survival of *E. coli* in 0.7% DMSO in saline, when exposed to 100 J/cm^2 light dose (56 mW/cm^2, 30 min) *vs.* the dye concentrations.

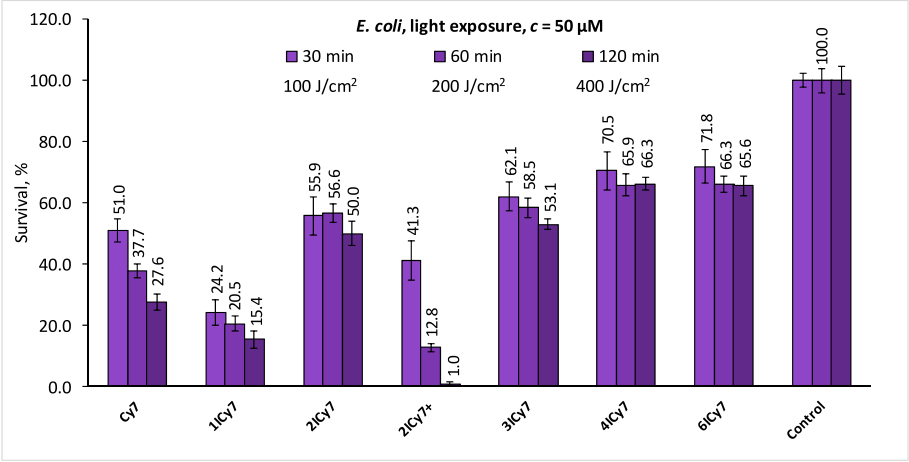

Fig. 7. Survival of *E. coli* at 50 μM dye concentrations in 0.7% DMSO in saline, when exposed to 100 J/cm^2 (30 min), 200 J/cm^2 (60 min), and 400 J/cm^2 (120 min) light doses.

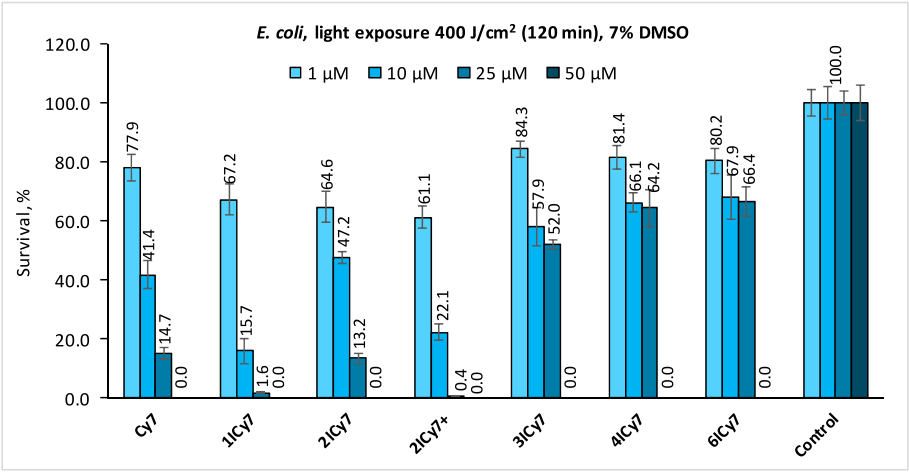

Fig. 8. Survival of *E. coli* in 7% DMSO in saline, when exposed to 400 J/cm^2 light dose (56 mW/cm^2, 120 min) *vs.* the dye concentrations.

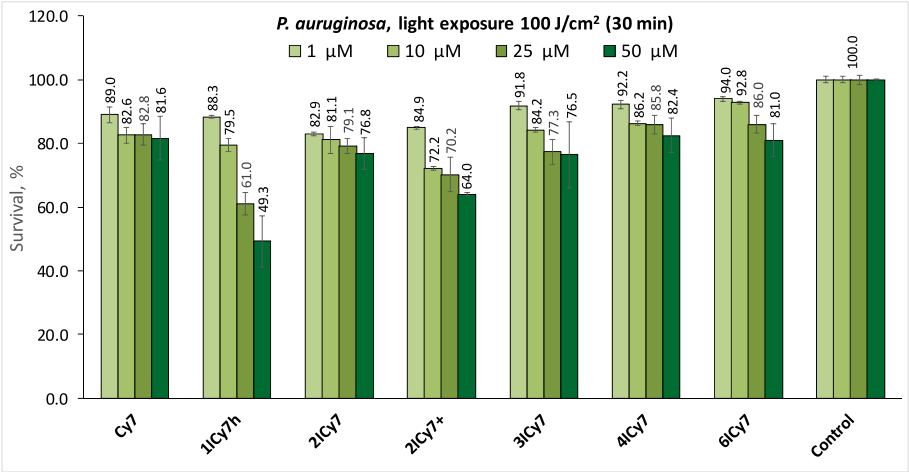

Fig. 9. Survival of *P. aeruginosa* in 0.7% DMSO in saline, when exposed to 100 J/cm^2 light dose (56 mW/cm^2, 30 min) *vs.* the dye concentrations.

4. Conclusions

A series of near-IR heptamethine cyanine dyes containing up to six iodine atoms and an aliphatic carboxylic group was synthesized; their spectral properties and ability for photodynamic eradication of *S. aureus*, *E. coli* and *P. aeruginosa* pathogens were investigated.

The increasing of the number of iodine atoms has an unexpected and ambiguous phototoxic effect on these bacteria, which is connected with

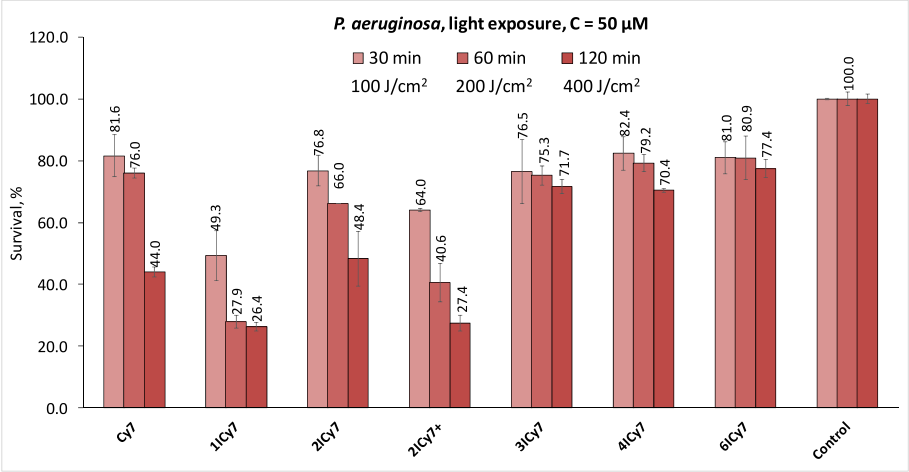

Fig. 10. Survival of *P. aeruginosa* at 50 μM dye concentrations in 0.7% DMSO in saline, when exposed to 100 J/cm^2 (30 min), 200 J/cm^2 (60 min), and 400 J/cm^2 (120 min) light doses.

two opposite factors: (i) increasing the spin–orbit coupling and the rates of reactive species generation and (ii) dye aggregation causing the reduced dye uptake (such a correlation was also noted in Ref. [46]) that, supposedly, is followed by decreased rates of reactive species generation. As a result, the increase of the number of iodine atoms up to two in the series of zwitterionic cyanines increases the efficacy of *S. aureus* eradication; then the efficacy remains almost unchanged for the two-, three- and four-iodinated dyes and diminishes in the case of the hexa-iodinated cyanine. At the same time, the mono-iodinated heptamethine cyanine causes the most pronounced phototoxic effect to *E. coli* and *Ps. aeruginosa*. An additional positive charge contributed by a triethylammonium group decreases efficacy of the dye towards *S. aureus* but improves eradication of *E. coli* and *Ps. aeruginosa*.

We believe that the developed dyes will be effective for treatment of other bacteria, viruses and cancer cells. The presence of carboxylic function potentially enables further binding of these dyes to various carriers.

CRediT authorship contribution statement

Olga Semenova: Spectral characterization, biological experiments with bacteria (APDT, cell uptake). **Dmytro Kobzev:** Synthesis. **Fares Yazbak:** Growth and preparation of bacteria. **Faina Nakonechny:** Analysis of cell survival, supervision of biological experiments. **Olga Kolosova:** Measurements of the quantum yield of singlet oxygen formation. **Anatoliy Tatarets:** Synthesis and supervision of synthetic work. **Gary Gellerman:** Writing the paper. **Leonid Patsenker:** General supervision, data analysis, and writing the paper.

Declaration of competing interest

The authors declare that they have no known competing financial interests or personal relationships that could have appeared to influence the work reported in this paper.

Acknowledgements

This work was supported by the Israel Scientific Foundation (ISF), project 810/18 and the Ariel University, Israel (Joint Research Project between Ariel University and Florida Atlantic University), FAU project RA2000000056. Leonid Patsenker is thankful to the Center for Absorption in Science of the Ministry of Immigrant Absorption of Israel for the financial support under the KAMEA program. Gary Gellerman is thankful to the Gale Foundation for the generous donation to support this work. Anatoliy Tatarets is thankful to the NAS of Ukraine (project 0120U102660). Authors are grateful to Dr. Vered Marks (Ariel University) for the measurements of NMR spectra.

Appendix A. Supplementary data

Supplementary data to this article can be found online at https://doi.org/10.1016/j.dyepig.2021.109745.

References

[1] Matsushima Y, Yashima A, Fukaya M, Shirakawa S, Ohshima T, Kawai T, et al. Effects of antimicrobial photodynamic therapy on organic solution and root surface in vitro. Antibiotics 2021;10:1–10. https://doi.org/10.3390/antibiotics10020101.
[2] Pinto AP, Rosseti IB, Carvalho ML, da Silva BGM, Alberto-Silva C, Costa MS. Photodynamic antimicrobial chemotherapy (PACT), using Toluidine blue O inhibits the viability of biofilm produced by *Candida albicans* at different stages of development. Photodiagnosis Photodyn Ther 2018;21:182–9. https://doi.org/10.1016/j.pdpdt.2017.12.001.
[3] Torabi S, Joharchi K, Kalhori KAM, Sohrabi M, Fekrazad R. Evaluation of antimicrobial photodynamic therapy on wounds infected by *Staphylococcus aureus* in animal models. Photodiagnosis Photodyn Ther 2021;33:102092. https://doi.org/10.1016/j.pdpdt.2020.102092.
[4] Shi H, Sadler PJ. How promising is phototherapy for cancer? Br J Canc 2020;123:871–3. https://doi.org/10.1038/s41416-020-0926-3.
[5] Li X, Lovell JF, Yoon J, Chen X. Clinical development and potential of photothermal and photodynamic therapies for cancer. Nat Rev Clin Oncol 2020;17(11):657–74. https://doi.org/10.1038/s41571-020-0410-2.
[6] Dias LD, Blanco KC, Bagnato VS. COVID-19: beyond the virus. The use of photodynamic therapy for the treatment of infections in the respiratory tract. Photodiagnosis Photodyn Ther 2020;31:101804. https://doi.org/10.1016/j.pdpdt.2020.101804.
[7] Liang Y, Lu LM, Chen Y, Lin YK. Photodynamic therapy as an antifungal treatment (Review). Exp Ther Med 2016;12:23–7. https://doi.org/10.3892/etm.2016.3336.
[8] Chang K, Tang Y, Fang X, Yin S, Xu H, Wu C. Incorporation of porphyrin to π-conjugated backbone for polymer-dot-sensitized photodynamic therapy. Biomacromolecules 2016;17(6):2128–36. https://doi.org/10.1021/acs.biomac.6b00356.
[9] Afonso SG, de Salamanca RE, Batlle AM del C. The photodynamic and non-photodynamic actions of porphyrins. Braz J Med Biol Res 1999;32(3):303–10. https://doi.org/10.1590/S0100-879X1999000300002.
[10] Li X, Zheng BD, Peng XH, Li SZ, Ying JW, Zhao Y, Huang JD, Yoon J. Phthalocyanines as medicinal photosensitizers: developments in the last five years. Coord Chem Rev 2019;379:147–60. https://doi.org/10.1016/j.ccr.2017.08.003.
[11] Li X, Yu S, Lee Y, Guo T, Kwon N, Lee D, Yeom SC, Cho Y, Kim G, Huang JD, Choi S, Nam KT, Yoon J. In Vivo albumin traps photosensitizer monomers from self-assembled phthalocyanine nanovesicles: a facile and switchable theranostic approach. J Am Chem Soc 2019;141(3):1366–72. https://doi.org/10.1021/jacs.8b12167.
[12] Li X, Lee D, Huang JD, Yoon J. Phthalocyanine-assembled nanodots as photosensitizers for highly efficient typeI photoreactions in photodynamic therapy. Angew Chem Int Ed 2018;57(31):9885–90. https://doi.org/10.1002/anie.201806551.
[13] Chinna Ayya Swamy P, Sivaraman G, Priyanka RN, Raja SO, Ponnuvel K, Shanmugpriya J, et al. Near Infrared (NIR) absorbing dyes as promising photosensitizer for photodynamic therapy. Coord Chem Rev 2020;411:213233. https://doi.org/10.1016/j.ccr.2020.213233.

[14] Shi C, Wu JB, Pan D. Review on near-infrared heptamethine cyanine dyes as theranostic agents for tumor imaging, targeting, and photodynamic therapy. J Biomed Opt 2016;21:050901. https://doi.org/10.1117/1.jbo.21.5.050901.
[15] van Straten D, Mashayekhi V, de Bruijn HS, Oliveira S, Robinson DJ. Oncologic photodynamic therapy: basic principles. Current clinical status and future directions. Cancers (Basel) 2017;9(2):19. https://doi.org/10.3390/cancers9020019.
[16] Omar GS, Wilson M, Nair SP. Lethal photosensitization of wound-associated microbes using indocyanine green and near-infrared light. BMC Microbiol 2008;8:111. https://doi.org/10.1186/1471-2180-8-111.
[17] Feng L, Chen W, Ma X, Liu SH, Yin J. Near-infrared heptamethine cyanines (Cy7): from structure, property to application. Org Biomol Chem 2020;18:9385–97. https://doi.org/10.1039/d0ob01962c.
[18] Thavornpradit S, Usama SM, Park GK, Shrestha JP, Nomura S, Baek Y, et al. QuatCy: a heptamethine cyanine modification with improved characteristics. Theranostics 2019;9(10):2856–67. https://doi.org/10.7150/thno.33595.
[19] Lange N, Szlasa W, Saczko J, Chwiłkowska A. Potential of cyanine derived dyes in photodynamic therapy. Pharmaceutics 2021;13(6):818. https://doi.org/10.3390/pharmaceutics13060818.
[20] Bilici K, Cetin S, Aydındogan E, Yagci Acar H, Kolemen S. Recent advances in cyanine-based phototherapy agents. Front Chem 2021;9:707876. https://doi.org/10.3389/fchem.2021.707876.
[21] Chi J, Ma Q, Shen Z, Ma C, Zhu W, Han S, et al. Targeted nanocarriers based on iodinated-cyanine dyes as immunomodulators for synergistic phototherapy. Nanoscale 2020;12:11008–25. https://doi.org/10.1039/c9nr10674j.
[22] Cao J, Chi J, Xia J, Zhang Y, Han S, Sun Y. Iodinated cyanine dyes for fast near-infrared-guided deep tissue synergistic phototherapy. ACS Appl Mater Interfaces 2019;11:25720–9. https://doi.org/10.1021/acsami.9b07694.
[23] Ebaston TM, Nakonechny F, Talalai E, Gellerman G, Patsenker L. Iodinated xanthene-cyanine NIR dyes as potential photosensitizers for antimicrobial photodynamic therapy. Dyes Pigments 2021;184:108854. https://doi.org/10.1016/j.dyepig.2020.108854.
[24] Bokan M, Nakonechny F, Talalai E, Kobzev D, Gellerman G, Patsenker L. Photodynamic effect of novel hexa-iodinated quinono-cyanine dye on *Staphylococcus aureus*. Photodiagnosis Photodyn Ther 2020;31:101866. https://doi.org/10.1016/j.pdpdt.2020.101866.
[25] Cahan R, Swissa N, Gellerman G, Nitzan Y. Photosensitizer-antibiotic conjugates: a novel class of antibacterial molecules. Photochem Photobiol 2010;86:418–25. https://doi.org/10.1111/j.1751-1097.2009.00674.x.
[26] Wang Z, Ivanov M, Gao Y, Bussotti L, Foggi P, Zhang H, et al. Spin-orbit charge-transfer intersystem crossing (ISC) in compact electron donor-acceptor dyads: ISC mechanism and application as novel and potent photodynamic therapy reagents. Chem Eur J 2020;26:1091–102. https://doi.org/10.1002/chem.201904306.
[27] Abrahamse H, Hamblin MR. New photosensitizers for photodynamic therapy. Biochem J 2016;473:347–64. https://doi.org/10.1042/BJ20150942.
[28] Liu H, Yin J, Xing E, Du Y, Su Y, Feng Y, et al. Halogenated cyanine dyes for synergistic photodynamic and photothermal therapy. Dyes Pigments 2021;190:109327. https://doi.org/10.1016/j.dyepig.2021.109327.
[29] Atchison J, Kamila S, Nesbitt H, Logan KA, Nicholas DM, Fowley C, et al. Iodinated cyanine dyes: a new class of sensitisers for use in NIR activated photodynamic therapy (PDT). Chem Commun 2017;53:2009. https://doi.org/10.1039/c6cc09624g. –12.
[30] Alberto ME, De Simone BC, Sicilia E, Toscano M, Russo N. Rational design of modified oxobacteriochlorins as potential photodynamic therapy photosensitizers. Int J Mol Sci 2019;20(8):2002. https://doi.org/10.3390/ijms20082002.
[31] Parker CA. Photoluminescence of solutions. Amsterdam, London, New York: Elsevier; 1968.
[32] Štacková L, Muchová E, Russo M, Slavíček P, Štacko P, Klán P. Deciphering the structure-property relations in substituted heptamethine cyanines. J Org Chem 2020;85:9776–90. https://doi.org/10.1021/acs.joc.0c01104.
[33] Ishchenko AA. Structure and spectral-luminescent properties of polymethine dyes. Russ Chem Rev 1991;60:865–84. https://doi.org/10.1070/rc1991v060n08abeh001116.
[34] Levitus M, Ranjit S. Cyanine dyes in biophysical research: the photophysics of polymethine fluorescent dyes in biomolecular environments. Q Rev Biophys 2011;44:123–51. https://doi.org/10.1017/S0033583510000247.
[35] Smith GJ. The effects of aggregation on the fluorescence and the triplet state yield of hematoporphyrin. Photochem Photobiol 1985;41:123–6. https://doi.org/10.1111/j.1751-1097.1985.tb03459.x.
[36] N-Dimethylaniline N. Sigma-aldrich. Safety data sheet, https://www.sigmaaldrich.com/IL/en/sds/aldrich/515124. [Accessed 1 August 2021]. accessed.
[37] Chemistry: 4-iodo-N,N-dimethylaniline. N-dimethylaniline; 2021. https://handwiki.org/wiki/Chemistry:4-Iodo-N. [Accessed 1 August 2021]. accessed.
[38] Jorge K. Soft drinks. Chemical composition. In: Caballero B, Finglas P, Toldrá F, editors. Encyclopedia of food sciences and nutrition. Academic Press; 2003. p. 5346–52. https://doi.org/10.1016/b0-12-227055-x/01101-9.
[39] 4-Iodobenzoic acid. https://www.chemicalbook.com/ChemicalProductProperty_EN_CB4374473.htm. [Accessed 1 August 2021]. accessed.
[40] 2,3,5-tri-iodobenzoic acid. PPDB: Pesticide Properties DataBase. University of Hertfordshire. http://sitem.herts.ac.uk/aeru/ppdb/en/Reports/2941.htm, [accessed 4 June 2021]. Lewis KA, Tzilivakis J, Warner DJ, Green A. An international database for pesticide risk assessments and management. Hum Ecol Risk Assess 2016;22:1050–1064. https://doi.org/10.1080/10807039.2015.1133242.
[41] Reddi BAJ. Why is saline so acidic (and does it really matter?). Int J Med Sci 2013;10:747–50. https://doi.org/10.7150/ijms.5868.
[42] Dean JA. Handbook of organic chemistry. New York, NY: McGraw-Hill Book Co.; 1987. p. 8–45.
[43] Riddick JA, Bunger WB, Sakano TK. Techniques of chemistry. In: Organic Solvents. Physical properties and methods of purification. fourth ed., vol. II. New York, NY: John Wiley and Sons; 1985.
[44] Zhao B, He YY, Chignell CF, Yin JJ, Andley U, Roberts JE. Difference in phototoxicity of cyclodextrin complexed fullerene [$(\gamma\text{-CyD})_2/C_{60}$] and its aggregated derivatives toward human lens epithelial cells. Chem Res Toxicol 2009;22:660–7. https://doi.org/10.1021/tx800478u.
[45] Ungati H, Govindaraj V, Mugesh G. The remarkable effect of halogen substitution on the membrane transport of fluorescent molecules in living cells. Angew Chem 2018;130:9127–31. https://doi.org/10.1002/ange.201804128.
[46] Sharma S, Dube A, Bose B, Gupta PK. Pharmacokinetics and phototoxicity of purpurin-18 in human colon carcinoma cells using liposomes as delivery vehicles. Canc Chemother Pharmacol 2006;57:500–6. https://doi.org/10.1007/s00280-005-0072-x.